Author's Accepted Manuscript

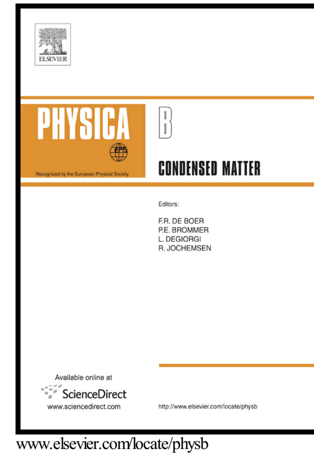

www.elsevier.com/locate/physb

Frequency and electric field controllable photodevice: FYTRONIX DEVICE

A. Tataroğlu, Abdullah G. Al-Sehemi, Mehmet Özdemir, Resul Özdemir, Hakan Usta, Ahmed A. Al-Ghamdi, W.A. Farooq, F. Yakuphanoglu

PII: S0921-4526(17)30272-7
DOI: http://dx.doi.org/10.1016/j.physb.2017.05.046
Reference: PHYSB309970

To appear in: *Physica B: Physics of Condensed Matter*

Received date: 14 May 2017
Revised date: 23 May 2017
Accepted date: 24 May 2017

Cite this article as: A. Tataroğlu, Abdullah G. Al-Sehemi, Mehmet Özdemir, Resul Özdemir, Hakan Usta, Ahmed A. Al-Ghamdi, W.A. Farooq and F. Yakuphanoglu, Frequency and electric field controllable photodevice FYTRONIX DEVICE, *Physica B: Physics of Condensed Matter* http://dx.doi.org/10.1016/j.physb.2017.05.046

This is a PDF file of an unedited manuscript that has been accepted fo publication. As a service to our customers we are providing this early version o the manuscript. The manuscript will undergo copyediting, typesetting, an review of the resulting galley proof before it is published in its final citable form Please note that during the production process errors may be discovered whic could affect the content, and all legal disclaimers that apply to the journal pertain

ACCEPTED MANUSCRIPT

Frequency and electric field controllable photodevice: FYTRONIX DEVICE

A. Tataroğlu[a], Abdullah G. Al-Sehemi[b,d], Mehmet Özdemir[e], Resul Özdemir[e], Hakan Usta[e], Ahmed A. Al-Ghamdi[f], W. A. Farooq[g], F. Yakuphanoglu[h*]

[a]Department of Physics, Faculty of Science, Gazi University, Ankara, Turkey
[b]Department of Chemistry, Faculty of Science, King Khalid University, Abha 61413, P.O. Box 9004, Saudi Arabia
[c]Research Center for Advanced Materials Science, King Khalid University, Abha 61413, P.O. Box 9004, Saudi Arabia
[d]Unit of Science and Technology, Faculty of Science, King Khalid University, Abha 61413,P.O. Box 9004, Saudi Arabia
[e]Department of Materials Science and Nanotechnology Engineering, Kayseri, Turkey
[f]Department of Physics, Faculty of Sciences, King Abdul Aziz University, Jeddah, Saudi Arabia
[g]Department of Physics and Astronomy, College of Science, King Saud University, Riyadh, Saudi Arabia
[h]Department of Physics, Faculty of Arts and Sciences, Firat University, 23169 Elazig, Turkey

[*]Corresponding author. fyhanoglu@firat.edu.tr (F.Yakuphanoglu)

Abstract

Al/p-Si/BODIPY/Al diode was fabricated by forming BODIPY organic layer on p-Si having ohmic contact. The electrical and photoresponse properties of the prepared diode were investigated in detail. The current-voltage (I-V) measurements were performed under dark and various illumination intensities. It is observed that the photocurrent under illumination is higher than the dark current. The transient measurements indicate that the device exhibits both photodiode and photocapacitor behavior. We called this device as FYTRONIX device. The photoresponse behavior of the FYTRONIX device is controlled simultaneously by frequency and electric field. The FYRONIX device can be used as a photoresponse sensor in optoelectronic applications.

Keywords: *BODIPY; organic thin film; Photodiode; Photoresponse device*

Accepted manuscript

1. Introduction

BODIPY (4,4-difluoro-4-bora-3a,4a-diaza-sindacene) is a highly electron-deficient molecular building block, which is considered as “porphyrin's little sister”. Since its discovery in 1960s, it has fostered a significant improvement in structural versatility in the field of organic chemistry, and a great number of molecules and polymers has been developed and studied in a variety of applications such as chemosensors, fluorescent switches, electroluminescent devices, and biochemical labeling [1-5]. To this end, although the structural and electronic properties of BODIPY π-core offer unique advantages such as structural co-planarity, high dipole-moment and energetically low lowest energy unoccupied molecular orbital (LUMO) level, its semiconducting characteristics has remained a relatively unexplored research field. Only, in the recent years, interest in semiconductor compounds embedding BODIPY as key π-building block has increased. To this end, some of us has recently reported the first BODIPY-based *n*-type molecular semiconductor in the literature, BDY-3T-BDY, which carries BODIPY π-acceptor units at molecular termini and terthiophene donor unit as the central π-core. The low LUMO energy level (-3.7 eV) and good solubility of this semiconductor has enabled the solution-based fabrication of *n*-channel organic field-effect transistors (OFETs) [6-7]. in bottom-gate/top-contact device geometry with electron mobilities of 3×10^{-4} $cm^2/V\cdot s$ and impressive I_{on}/I_{off} ratios of 10^7-10^8. To the best of our knowledge, this was the first demonstration of *n*-channel semiconductivity for a BODIPY-based compound demonstrating that π-extension along BODIPY’s meso-position leads to electron-transport, which is in sharp contrast to our earlier findings and other groups’ observations as well that π-extension through aromatic substitutions on BODIPY’s 2,6-positions leads to hole-transport [6-11]. In these studies, BODIPY core has proven itself as a promising π-

Accepted manuscript

ACCEPTED MANUSCRIPT

conjugated building block with superior solution processibility and good charge-transport behavior. Therefore, further electrical and optical characterizations to investigate these BODIPY compounds are highly desirable to reveal their full potential in various optoelectronic applications [13].

In this paper, we fabricated Al/p-Si/ BDY-3T-BDY /Al diode and studied its electrical and photoresponse properties. These properties were investigated by illumination-dependent current-voltage and the frequency-dependent admittance measurements.

2. Experimental details

2.1. Synthesis processes of BDY-3T-BDY

2.1.1. Synthesis of 5-bromo-2-thiophenecarbaldehyde

To a solution of 2-thiophenecarboxaldehyde (6.0 g, 53.5 mol) in anhydrous $CHCl_3$ (125 mL), N-bromosuccinimide (10.4 g, 58.9 mmol) was slowly added, and then the reaction mixture was stirred for overnight at room temperature. The reaction mixture was extracted with $CHCl_3$, and the organic phase was washed with deionized water, dried over Na_2SO_4, filtered, and evaporated to dryness to give the crude product. Column chromatography was performed on silica gel using $CHCl_3$ as the eluent, which affords the pure product as a colorless oil (10.0 g, 98%). ^{1}H NMR (400 MHz, $CDCl_3$): δ 7.20 (d, H, J = 4.0 Hz), 7.53 (d, H, J = 8.0 Hz), 9.79 (s, H).

2.1.2. Synthesis of 8-(2-bromothien-5-yl)-3,5-dimethyl-4,4-difluoro-4-bora-3a,4a-diaza-s-indacene (BDY-T-Br)

Accepted manuscript

ACCEPTED MANUSCRIPT

Trifluoroacetic acid (TFA) (4 drops) was added under nitrogen to a solution of 5-bromo-2-thiophenecarbaldehyde (**1**) (1.05 g, 5.49 mmol) and 2-methylpyrrole (**2**) (1.0 g, 12.42 mmol) in degassed CH_2Cl_2 (330 mL), and the mixture was stirred at ambient temperature overnight. 2,3-dichloro-5,6-dicyano-1,4-benzoquinone (DDQ) (1.25 g, 5.49 mmol) was then added to this solution, and the reaction mixture was stirred for additional 3 h. Finally, N,N-diisopropylethylamine $(i\text{-}Pr)_2EtN$ (3.9 g, 30.08 mmol) and boron trifluoride diethyl etherate ($BF_3{\cdot}Et_2O$) (2.72 g, 19.05 mmol) were added, and the reaction mixture was stirred for 2 h. The reaction mixture was poured into water and extracted with CH_2Cl_2. The organic phase was dried over Na_2SO_4, filtered, and evaporated to dryness to give a crude product. The crude was purified by column chromatography on silica gel using CH_2Cl_2:Hexanes (2:1) as the eluent, which yields the pure product as a crystalline red solid (1.0 g, 48% yield). m.p. 132-133 °C. ^1H NMR (400 MHz, $CDCl_3$): δ 2.68 (s, 6H), 6.32 (d, 2H, J=4.0 Hz), 7.05 (d, 2H, J = 4.0 Hz), 7.19 (m, 2H). ^{13}C NMR (100 MHz, $CDCl_3$): 15.0, 116.9, 119.7, 130.1, 130.6, 131.7, 133.2, 133.9, 136.1, 158.2.

2.1.3. Synthesis of 5,5''-Bis(3,5-dimethylBODIPY-8-yl)-2,2':5',2''-Terthiophene (BDY-3T-BDY)

The reagents BDY-T-Br (0.72 g, 1.88 mmol), 2,5-bis(trimethylstannyl)thiophene (0.36 g, 0.90 mmol), and $Pd(PPh_3)_2Cl_2$ (0.02 g, 26.7 μmol) were suspended in anhydrous toluene (45 mL) and the reaction mixture was heated at 110 °C under nitrogen for 48 h. Then, the reaction mixture was cooled down to room temperature and evaporated to dryness. The crude product was filtered and washed with methanol to give a dark crude solid, which was purified by column chromatography on silica gel with $CHCl_3$:Hexanes (1:1) as the eluent to give final pure product as a dark red solid (0.33 g, 54% yield). $T_{decomposition} > 250$ °C. ^1H NMR (400 MHz, $CDCl_3$): δ 2.68 (s, 6H), 6.35 (m, 2H), 7.15(m,

Accepted manuscript

ACCEPTED MANUSCRIPT

2H), 7.22-7.42 (m, 3H). ^{13}C NMR (100 MHz, $CDCl_3$): 15.0, 119.5, 119.7, 124.4, 124.5, 125.0, 125.2, 125.7, 130.1, 132.6, 132.8, 133.8, 134.7, 140.4, 157.6, 157.7, 158.1. MS(MALDI-TOF) m/z (M^+): calcd. for $C_{34}H_{26}B_2F_4N_4S_3$: 684.14, found: 684.96 $[M+H]^+$, 664.88 $[M-F]^+$, 602.78 $[M-4\times CH_3-F]^+$, 583.70 $[M-4\times CH_3-2\times F]^+$. Anal.calcd. for $C_{34}H_{26}B_2F_4N_4S_3$: C, 59.67; H, 3.83; N, 8.19, Found: C, 59.83; H, 4.07; N, 7.89.

The synthesis of BDY-3T-BDY is shown in Scheme 1 and it's synthesis was performed in three steps in accordance with our previous reported procedure [1].

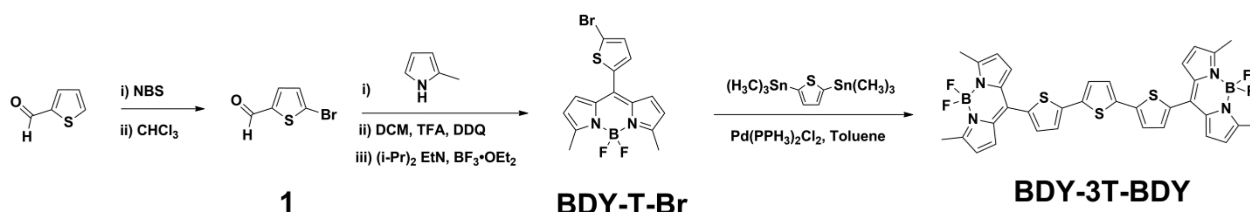

Scheme 1. Synthesis of BDY-3T-BDY

Accepted manuscript

2.2. Fabrication of Al/p-Si/ BDY-3T-BDY /Al Diode

The diode was prepared using p-type silicon wafer and **BDY-3T-BDY** organic material. Firstly, a p-type silicon substrate was chemically cleaned using some chemical baths. After cleaning procedure, Al ohmic contact was prepared to p-Si wafer by thermal evaporating of Al and then, it was annealed at 570 ^{o}C for 5 min in nitrogen atmosphere.

After ohmic contact procedure, the solution of BDY-3T-BDY organic compound was prepared and the solution was drop coated on p-type silicon wafer and dried at 50 ^{o}C for 20 min. Al metal as a top contact was prepared on the organic layer having a diode contact area of 7.85×10^{-3}. Electrical measurements of the diode were carried out by using a FYtronix FYED-500 Electronic Device characterization system at room temperature.

3. Results and Discussion

3.1. Current-voltage (I-V) characteristics of the diode

The current-voltage (I-V) characteristics of the fabricated diode are shown in Fig.1. As seen in Fig.1, the current of the diode in lower forward bias voltages is increased exponentially. This indicates that the diode exhibited a rectifying behavior. This behavior can be analyzed by the conventional thermionic emission (TE) theory. According to TE theory, the relationship between current (I) and voltage (V) for forward biases of V > 3kT/q is given as [13-14],

$$I = I_o\left[\exp\left(\frac{q(V-IR_s)}{nkT}\right)-1\right] \quad (1)$$

where I_0 is the reverse saturation current, V is the applied bias voltage, R_s is the series resistance, n is the ideality factor, k is the Boltzman's constant, and T is the absolute temperature. I_0 is extracted from the straight line intercept of ln(I) at V=0 and is given by,

$$I_0 = AA^{*}T^{2}\exp\left(-\frac{q\Phi_b}{kT}\right) \quad (2)$$

where A is the diode area, Φ_b is the zero-bias barrier height, and A^* is the effective Richardson constant which is equal to 32 $A/cm^2.K^2$ for p-type Si. The Φ_b value is obtained from Eq. (2). The ideality factor (n) is extracted from the slope of the linear region of lnI-V plot, and its value should be 1 for ideal Schottky diode. From Eq. (1), the ideality factor can be written as

$$n = \frac{q}{kT}\left(\frac{dV}{d(\ln I)}\right) \quad (3)$$

Accepted manuscript

ACCEPTED MANUSCRIPT

The photoresponse properties of the Al/p-Si/BODIPY/Al diode was evaluated by measuring the I-V characteristics under illumination. Fig. 1 shows the semi-logarithmic forward and reverse bias I-V plots of the diode in dark and under various illumination intensities. As seen in Fig. 1, the diode shows a good rectifying behavior. Under illumination, photocurrent in reverse bias is higher than the dark current, and its value increases with increasing illumination intensity. This indicates that the diode exhibits a photoconducting behavior. This also explains that the resistance of the diode decreases with illumination. When a diode is illuminated, the electron-hole pairs are generated in the depletion region due to absorption of photons. The photogenerated charge carriers such as electrons and holes will create an additional current flow across the junction, and they must be added to the dark current [15-21]. In addition, under forward bias, no differences were observed between the dark and photocurrent.

Accepted Manuscript

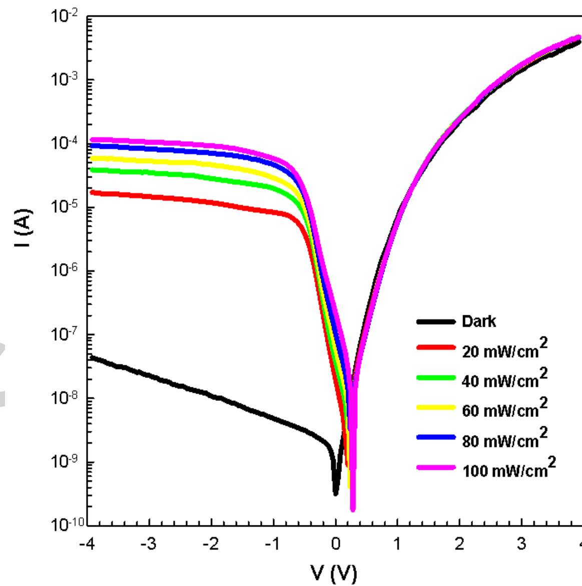

Fig. 1. The semi-logarithmic current-voltage (I-V) plots of the diode.

The value of ideality factor and barrier height for dark was found to be about 3.1 and 0.82 eV, respectively. This barrier height is found to be slightly increased from the vacuum

ACCEPTED MANUSCRIPT

level energy difference between Aluminum work function (4.3 eV) and the LUMO energy level of BDY-3T-BDY (-3.7 eV) probably due to the formation of interface dipoles.) For all illumination, the values of these parameters was found to be about 3.5 and 0.80 eV. The obtained n value is greater than 1. This can be attributed to the existence of the interface layer and interface states, barrier inhomogeneous, and series resistance [1,2,22-24].

Additionally, Norde method is an alternative method to find out the magnitude of barrier height. According to this method, Norde's function, F(V), is plotted against voltage (V) and is expressed as [25,26],

$$F(V) = \frac{V}{\gamma} - \frac{kT}{q}\ln\left(\frac{I}{AA^{*}T^{2}}\right)$$

(4)

where γ is an integer greater than the ideality factor. The barrier height is given by

$$\Phi_b = F(V_{\min}) + \frac{V_{\min}}{\gamma} - \frac{kT}{q}$$

(5)

where $F(V_{min})$ is the minimum value of F(V) and V_{min} is the corresponding voltage. The series resistance is given by

$$R_s = \frac{kT(\gamma - n)}{qI_{\min}} \tag{6}$$

Fig. 2 shows plots of F(V) for dark and 100 mW/cm^2. As seen in Fig. 2, the F(V) plots give a minimum point.. The barrier height values for dark and 100 mW/cm^2 were found to be 0.86 and 0.84 eV, respectively. These values are in good agreement with the values obtained from the I-V method. For these conditions, the series resistance values were found to be 171 kΩ and 122 kΩ. This indicates that the series resistance decreases with illumination.

Accepted manuscript

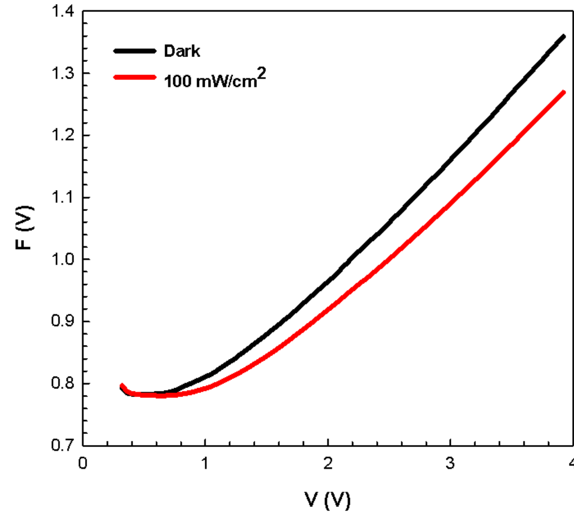

Fig. 2. Plots of F(V) vs. V of the diode.

The photoresponse properties and photoconduction mechanism of the diode can be analyzed by the following relation [27,28],

$$I_{ph} = AP^{m} \tag{7}$$

where I_{ph} is the photocurrent, A is a constant, m is an exponent and P is the illumination intensity. The m value is extracted from the slope of log (I_{Ph}) versus log (P) plot. Values of m between 0.5 and 1 indicate the presence of a continuous distribution of localized states. A higher value of m indicates a lower density of the unoccupied trap level. A higher value of m indicates a lower density of the unoccupied trap level [28-31]. Fig. 3 shows the variation of photocurrent with various illumination intensities. The value of m is found to be 1.18. This m value indicates that the photoconduction mechanism of the diode exhibits a linear behavior.

Accepted manuscript

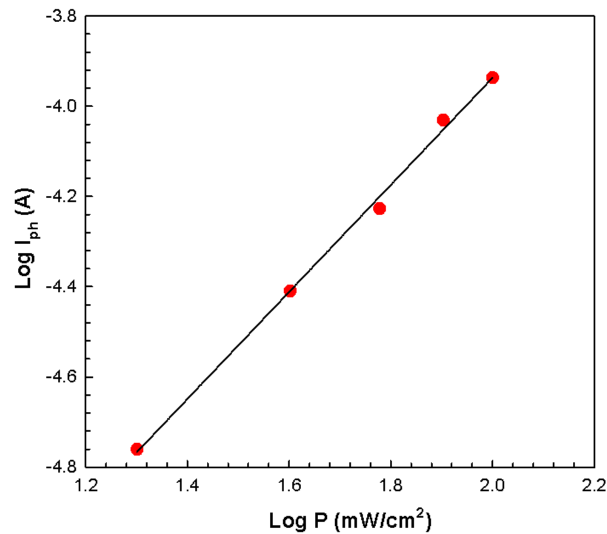

Fig. 3. Plot of log(I_{ph}) vs. log(P) of the diode (at -4 V).

3.2. Transient photocurrent/photocapacitance/photoconductance-time characteristics

To analyze the photoresponse stability of the diode, time-dependent transient photocurrent measurements were used. Fig. 4 shows the transient photocurrent-time plots of the diode. The photocurrent increases under illumination, and then decreases quickly when the illumination is turned off. The increase in photocurrent is due to the increase in the number of photogenerated charge carriers. The decrease in photocurrent is attributed to the trapping of the charge carriers in the deep levels [32-36].

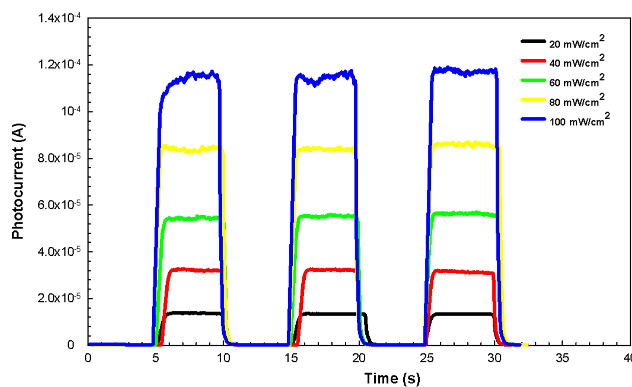

Fig. 4. Transient photocurrent-time plots under various illuminations.

Accepted manuscript

ACCEPTED MANUSCRIPT

The transient photocapacitance and photoconductance are a measure of the density of photogenerated carriers in the space charge region. Fig. 5(a) and (b) show the transient photocapacitance-time and photoconductance-time plots of the diode at 10 kHz, respectively. As seen in Fig. 5(a), in case of turning off the illuminating, the photocapacitance increases rapidly to a certain value. In case of turning off, the capacitance suddenly come back to initial value. Moreover, the photocapacitance value increases with increasing illumination intensity. As seen in Fig. 5(b), the photoconductance value decreases with increasing illumination intensity. These measurements suggest that the diode exhibits a photocapacitive behavior.

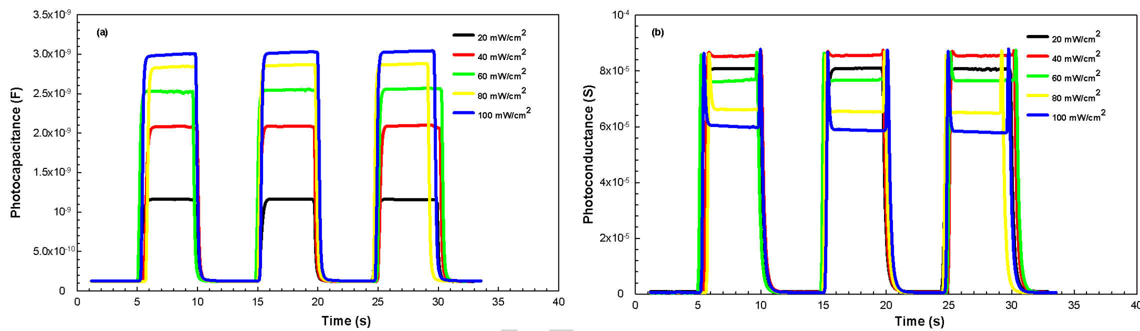

Fig. 5. Transient (a) photocapacitance-time (b) photoconductance-time plots at 10 kHz and under various illuminations.

Accepted Manuscript

3.3. Capacitance/conductance-voltage (C/G-V) characteristics

The capacitance-voltage (C-V) and conductance-voltage (G-V) plots at various frequencies are given in Fig. 6(a) and (b), respectively. As seen in these figures, in reverse bias region, the capacitance value decreases, while the conductance value increases with increasing frequency. In forward bias region, they do not change with frequency. The frequency dependence is attributed to the existence of interface states in the interface of the diode. At low frequencies, the interface states are very sensitive to the alternating current

signal (ac). But, their sensitivity decreases at high frequencies (f≥500 kHz). Therefore, the interface states cannot follow the ac signal at high frequencies and cannot contribute to the total capacitance of the diode [13,37-42].

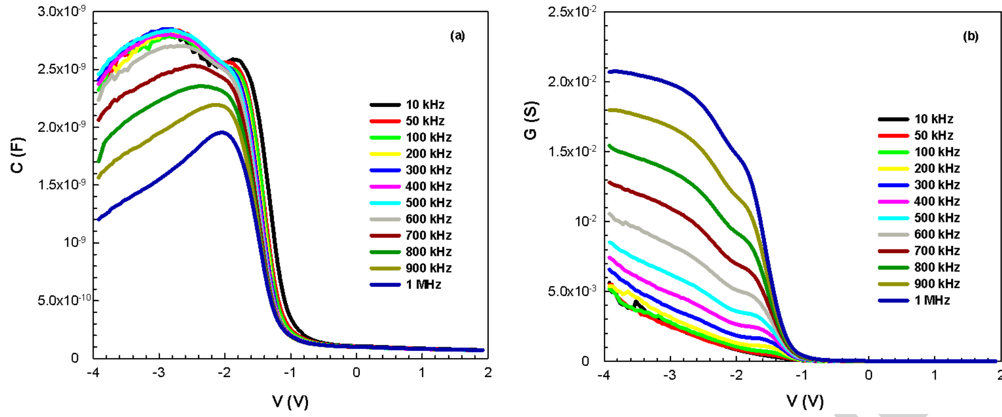

Fig. 6. (a) capacitance-voltage (C-V) and (b) conductance-voltage (G-V) plots at various frequencies.

The series resistance (R_s) of the diode is determined by the following the equation [37,43],

$$R_s = \frac{G_{ma}}{G_{ma}^2 + (\omega C_{ma})^2} \tag{8}$$

where C_{ma} and G_{ma} are the measured capacitance and conductance, respectively. The R_s-V plots at various frequencies are given in Fig. 7. As seen in Fig. 7, the R_s value decreases with increasing frequency. This behavior of R_s is result from the frequency dependence of interface charges. Also, in reverse bias region, the R_s-V plots give a peak. The magnitude of peaks is attributed to the particular distribution of interface states [40-44].

Accepted manuscript

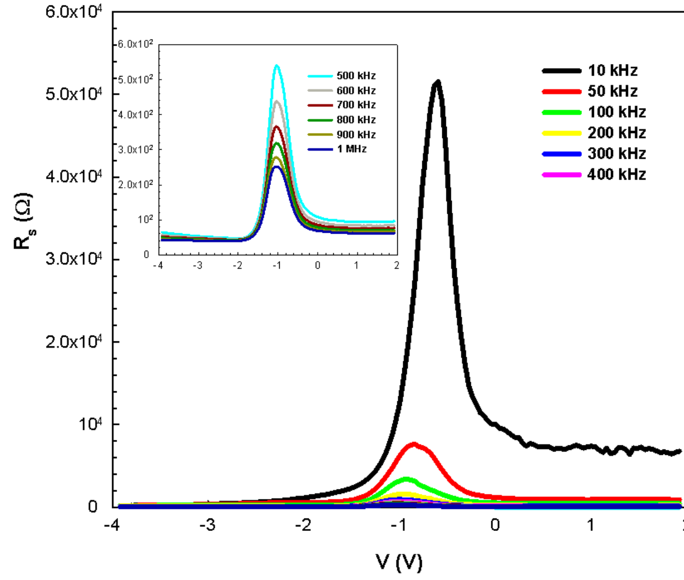

Fig. 7. The series resistance-voltage (R_s-V) plots at various frequencies.

The measured capacitance and conductance are affected by series resistance and corrected by the following equations [33,43,45],

$$C_{ADJ} = \frac{\left[G_m^2 + (\omega C_m)^2\right] C_m}{a^2 + (\omega C_m)^2} \tag{9}$$

$$G_{ADJ} = \frac{\left[G_m^2 + (\omega C_m)^2\right] a}{a^2 + (\omega C_m)^2} \tag{10}$$

and

$$a = G_m - \left[G_m^2 + (\omega C_m)^2\right] R_s \tag{11}$$

where C_{ADJ} and G_{ADJ} is the corrected capacitance and conductance, respectively. Fig. 8(a) and (b) show C_{ADJ}-V and G_{ADJ}-V plots at various frequencies, respectively. From Fig. 8(a), it is observed that the value of C_{ADJ} decreases with increasing frequency. As seen in Fig. 8(b), the value of G_{ADJ} increases with increasing frequency. Furthermore, the G_{ADJ}-V plots gives a peak in the reverse bias voltage. This peak is attributed to the existence of series resistance and interface states.

Accepted manuscript

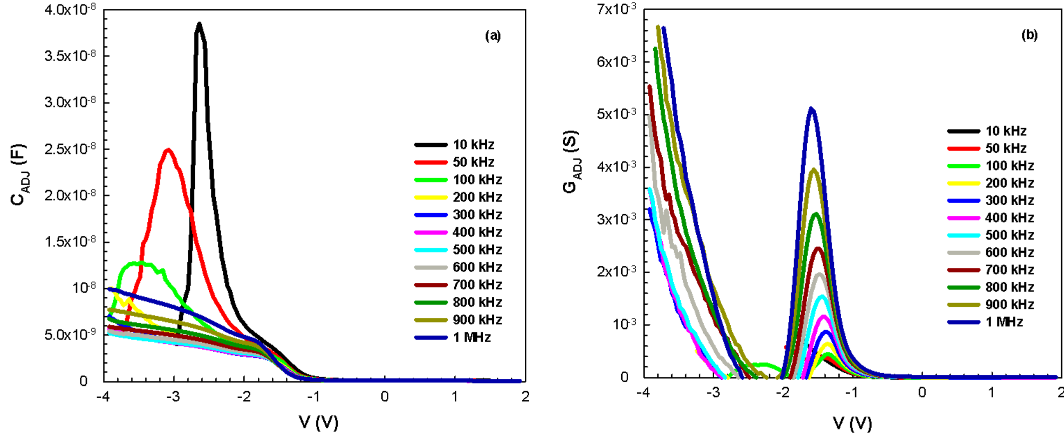

Fig. 8. (a) C_{ADJ}-V and (b) G_{ADJ}-V plots at various frequencies.

The interface state density (N_{ss}) can be determined by using Hill-Coleman method [46]. According to this method, the N_{ss} is given by,

$$N_{ss} = \frac{2}{qA} \left[\frac{(G_m/\omega)_{\max}}{((G_m/\omega)_{\max} C_{ox})^2 + (1 - C_m/C_{ox})^2} \right] \quad (12)$$

where $(G_m/\omega)_{max}$ is the maximum measured conductance and C_{ox} is the oxide capacitance. The variation of N_{ss} with frequency is given in Fig. 9. As seen in Fig. 9, the N_{ss} value decreases with increasing frequency. This behavior of N_{ss} is attributed to the decrease in numbers of interface charge carries.

Accepted manuscript

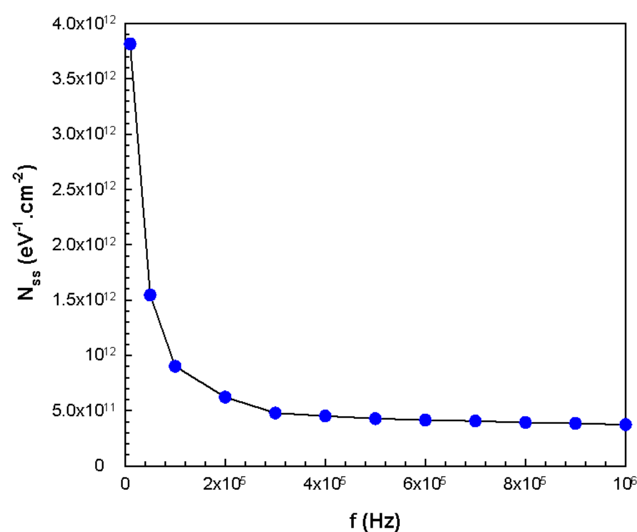

Fig. 9. Variation of N_{ss} with frequency

4. Conclusions

The electrical and photoresponse properties the Al/p-Si/BODIPY/Al diode with organic layer have been investigated by using I-V, C/G-V characteristics. The fabricated diode indicates a good rectifying behavior and exhibits photovoltaic behavior. The diode exhibited both photodiode and photocapacitor behavior. The obtained experimental results suggest that the prepared diode can be used as a photodiode in optoelectronic applications.

Acknowledgements

The authors extend their appreciation to the International Scientific Partnership Program ISPP at King Saud University for funding this research work through ISPP# 0046.

Accepted manuscript

ACCEPTED MANUSCRIPT

References

[1] M. Ozdemir, D. Choi, G. Kwon, Y. Zorlu, B. Cosut, H. Kim, A. Facchetti, C. Kim, H. Usta, ACS Appl. Mater. Interfaces 8 (2016) 14077-14087.

[2] A.C. Benniston, G. Copley, A. Harriman, D.B. Rewinska, R.W. Harrington, W.A. Clegg, J. Am. Chem. Soc. 130 (2008) 7174-7175.

[3] P. Bonaccorsi, M.C. Aversa, A. Barattucci, T. Papalia, F. Puntoriero, S. Campagna, Chem. Commun. 48 (2012) 10550-10552.

[4] L. Niu, Y. Guan, Y. Chen, L. Wu, C. Tung, Q. Yang, J. Am. Chem. Soc. 134 (2012) 18928-18931.

[5] A. Loudet, K. Burgess, Chem. Rev. 107 (2007) 4891-4932.

[6] Mehmet Ozdemir, Donghee Choi, Guhyun Kwon, Yunus Zorlu, Hyekyoung Kim, Myung-Gil Kim, SungYong Seo, Unal Sen, Murat Citir, Choongik Kim and Hakan Usta, RSC Adv., 2016, 6, 212–226

[7] Fabiano S., Usta H., Forchheimer R. , Crispin X. , Facchetti A., Berggren M., "Selective Remanent Ambipolar Charge Transport in Polymeric Field-Effect Transistors For High-Performance Logic Circuits Fabricated in Ambient", ADVANCED MATERIALS, vol.26, pp.7438-7443, 2014

[8] W. Liu, A. Tang, J. Chen, Y. Wu, C. Zhan, J. Yao, ACS Appl. Mater. Interfaces 6 (2014) 22496-22505.

[9] J.J. Chen, S.M. Conron, P. Erwin, M. Dimitriou, K. McAlahney, M.E. Thompson, ACS Appl. Mater. Interfaces 7 (2015) 662-669.

[10] D. Ji, L. Jiang, H Usta H., Yilmaz M.D., Avestro A., Boudinet D., Denti M., Zhao W., Stoddart J.F., Facchetti A., ADVANCED MATERIALS, vol.25, pp.4327-4334, 2013.

[11] Usta H., Yilmaz M.D., Avestro A., Boudinet D., Denti M., Zhao W., Stoddart J.F., Facchetti A., , ADVANCED MATERIALS, vol.25, pp.4327-4334, 2013

[12] Figa V., Chiappara C., Ferrante F., Casaletto M.P., Principato F., Cataldo S., et al., , JOURNAL OF MATERIALS CHEMISTRY C, vol.3, pp.5985-5994, 2015

Accepted manuscript

ACCEPTED MANUSCRIPT

[13] S.M. Sze, Physics of Semiconductor Devices, 2nd Ed., John Wiley& Sons, New York, 1981.

[14] B.L. Sharma, Metal-Semiconductor Schottky Barrier Junctions and Their Applications, Plenum Press, New York, 1984.

[15] J. Singh, Electronic and Optoelectronic Properties of Semiconductor Structures, Cambridge University Press, New York, 2003.

[16] I. Yun, Photodiodes-from Fundamentals to Applications, InTech, Croatia, 2012.

[17] R.O. Ocaya, A.G. Al-Sehemi, A.A. Al-Ghamdi, Farid El-Tantawy,F. Yakuphanoglu, J. Alloys Compd. 702 (2017) 520-530.

[18] G.M. Kumar, F. Xiao, P. Ilanchezhiyan, Sh. Yuldashev, T.W. Kang, RSC Adv. 6 (2016) 99631-99637.

[19] I. Orak, A. Kocyigit, A. Turut, J. Alloys Compd. 691 (2017) 873-879.

[20] C. Aksu Canbay, A. Tataroglu, A. Dere, Ahmed Al-Ghamdi, F. Yakuphanoglu, J. Alloys Compd. 688 (2016) 762-768.

[21] A. Chouket, B. Cherif, N.B. Salah, K. Khirouni, J. Appl. Phys. 114 (2013) 243105.

[22] R.T. Tung, Mater. Sci. Eng. R 35 (2001) 1-138.

[23] J.H. Werner, H.H. Guttler, J. Appl. Phys. 69 (1991) 1522-1533.

[24] R. Kumar, S. Chand, J. Mater. Sci.: Mater. Electron. 25 (2014) 4531-4537.

[25] H. Norde, J. Appl. Phys. 50 (1979) 5052-5054.

[26] K. Sato, Y. Yasumura, J. Appl. Phys. 58 (1985) 3655-3657.

[27] R.H. Bube, Photoconductivity of Solids, New York, Wiley, 1960.

[28] R. Singh, A.K. Narula, Appl. Phys. Lett. 71 (1997) 2845-2847.

[29] S. Kazim, V. Alia, M. Zulfequar, M.M. Haq, M. Husain, Physica B 393 (2007) 310-315.

[30] A. Rose, Concepts in Photoconductivity, Interscience, New York, 1963.

[31] F. Yakuphanoglu, K. Mensah-Darkwa, A.A. Al-Ghamdi, R.K. Gupta, W.A. Farooq, Microelectron. Eng. 160 (2016) 27-33.

[32] A. Tataroglu, O. Dayan, N. Ozdemir, Z. Serbetci, A.A. Al-Ghamdi, A. Dere, F. El-Tantawy, F. Yakuphanoglu, Dyes Pigments 132 (2016) 64-71.

[33] J.C. Moore, C.V. Thompson, Sensors 13(2013) 9921-9940.

Accepted manuscript

ACCEPTED MANUSCRIPT

[34] G. Cheng, X.Wu, B. Liu, B. Li, X. Zhang, Z. Dua, Appl. Phys. Lett. 99 (2011) 203105.

[35] R. Maiti, S. Manna, A. Midya, S.K. Ray, Optics Express 21 (2013) 26034-26043.

[36] A.A. Hendi, F. Yakuphanoglu, J. Alloys Compd. 665 (2016) 418-427.

[37] E.H. Nicollian, J.R. Brews, MOS Physics and Technology, Wiley, New York, 1982.

[38] A. Tataroglu, A.A. Al-Ghamdi, F. El-Tantawy, W.A. Farooq, F. Yakuphanoglu, Appl. Phys. A 122 (2016) 220-6.

[39] M. Sharma, S.K. Tripathi, Mater. Sci. Sem. Process. 41 (2016) 155-161.

[40] M. Soylu, M. Cavas, A.A. Al-Ghamdi, Z.H. Gafer, F. El-Tantawy, F.Yakuphanoglu, Solar Energy Mater. Solar Cells 124 (2014) 180-185.

[41] R. Padma, K. Sreenu, V.R.Reddy, J. Alloys Compd. 695 (2017) 2587-2596.

[42] S. Altındal, H. Uslu, J. Appl. Phys. 109 (2011) 074503.

[43] E.H. Nicollian, A. Goetzberger, Bell Syst. Tech. J. 46 (1967) 1055-1133.

[44] S. Karatas, A. Turut, Vacuum 74 (2004) 45-53.

[45] E.H. Nicollian, A. Goetzberger, A.D. Lopez, Solid-State Electron. 12 (1969) 937-944.

[46] W.A. Hill, C.C. Coleman, Solid-State Electron. 23 (1980) 987-993.

Accepted manuscript